ENGINEERING SOLID ELECTROLYTE/ELECTRODE INTERFACES FOR ALL SOLID-STATE LITHIUM-ION BATTERY

UNDERGRADUATE HONOR THESIS

JUNBIN CHOI

ADVISOR: DR. JUNG HYUN KIM

April, 2018

Department of Mechanical and Aerospace Engineering

The Ohio State University

In Partial Fulfillment of the Requirements

For Graduation with Distinction in Mechanical Engineering

Abstract

Nowadays, most commercialized portable electronic devices, such as cell-phones and laptops, use Li-ion batteries as their power source. Li-ion batteries are also being used by automotive companies to power electric vehicles (EVs). However, there is a strong need to make Li-ion batteries safer under abusive conditions, such as car accidents. To address this need, significant research has been recently conducted to utilize solid electrolytes in Li-ion battery cells for the next generation EV applications. In this study, I investigated several solid electrolyte and electrode materials to seek their optimal combinations in terms of chemical stabilities at electrolyte – electrode interfaces. The objective of this study is finding governing parameters that stabilize the interfaces and offer unhindered Li-ion transportations across the interfaces. Among various ceramic electrolyte materials, I selected $Li_{1+x}Al_xTi_{2-x}(PO_4)_3$ (LATP) based on its good chemical stability in air and moisture. First, I synthesized the LATP powder by using sol-gel method, followed by sintering at 850^{o}C for 5 h in air. The phase purity and particle morphology were characterized, respectively, by using X-ray diffractometer (XRD) and scanning electron microscopy (SEM). I investigated high-temperature stability between cathode materials and LATP by sintering their mixture in a range of 600^{o}C – 900^{o}C. The resulting powders were measured by XRD to identify their phase stabilities. This high-temperature sintering process is a necessary step for a fabrication of the solid-state batteries. Then, I examined electrochemical properties of the LATP – cathode composite by using coin-cells. In this presentation, I will discuss the effect of interfacial stabilities (i.e., LATP – cathode) on the physical and electrochemical properties.

Acknowledgements

Firstly, I give my special thanks to Dr. Jung-Hyun Kim for giving me an opportunity to participate in the undergraduate research program. Even though this battery field was relatively new for me, he kindly supported and encouraged me to get used to it. As a result, I finally decided to pursue doctoral degree in this field. Without his generous guidance, I would not have confidence and belief that have now, which I can make a great achievement in the future.

I also want to thank to Dr. Anne Co. She provided her lab for me and my colleagues to conduct experiments before Dr. Kim's lab was set up. It was first time for me to do the hand-on experiment and it was a great motive for me to get interested about the research. Also, Daniel Lyons, a graduate student in Dr. Co's lab provided $LiMn_2O_4$ reagent he synthesized.

Table of Contents

List of Figures

List of Tables

Chapter 1: Introduction

Lithium-ion battery(LIB) is refers to a type of rechargeable energy storage system. It utilizes chemical reactions, oxidation and reduction, to store energy. It consists of three main components: positive electrode(cathode), negative electrode(anode), and electrolyte between two electrodes. When discharging, lithium-ions embedded in the anode move toward cathode through electrolyte while dropping electrons from each lithium atoms. The electrons move from negative to positive electrode through wire and therefore, the current flows. In the meantime, lithium-ion migrate through electrolyte toward cathode. In case of charging, and external electric power source forces current flows in the opposite direction(negative to positive) and lithium-ion migrate from positive to negative. As a result, energy is stored at negative electrode.

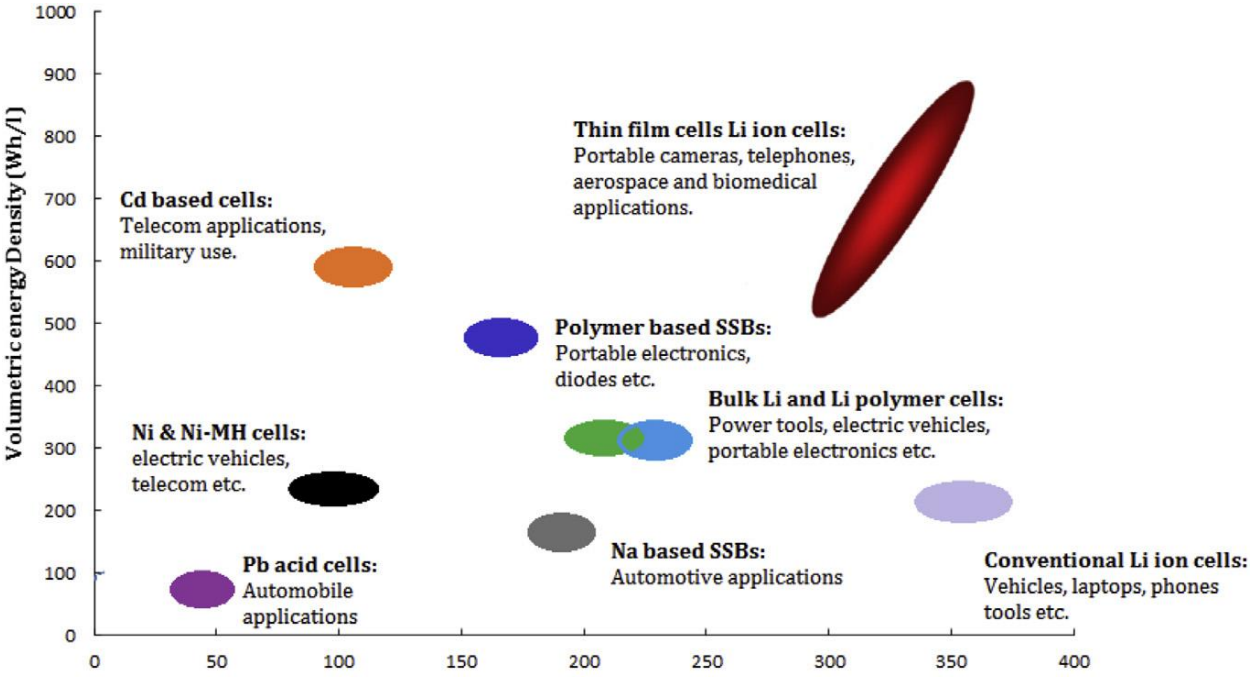

Figure 1 Capacities of different types of batteries and their respective applications [1]

Thanks to its higher energy capacity compared to the other types of rechargeable batteries, Li-ion batteries have been utilized as main power sources in broad areas, especially for portable electric devices. Moreover, like Chevrolet Bolt, Toyota Prius, and Tesla models, major automotive

companies have commercialized electric vehicles(EVs), which have LIB as their main powertrains. However, even though the LIB market is still growing and industries are improving their performance and stability, there are drawbacks that the conventional LIB must overcome for the next generation application. One of the main drawback is safety feature. The electrolyte materials in conventional Li-ion batteries are liquid state, and they are highly flammable. Therefore, damages on the batteries due to abusive condition can lead to life-threatening consequences such as an explosion of battery after a car clash. To avoid these consequences, industries have been

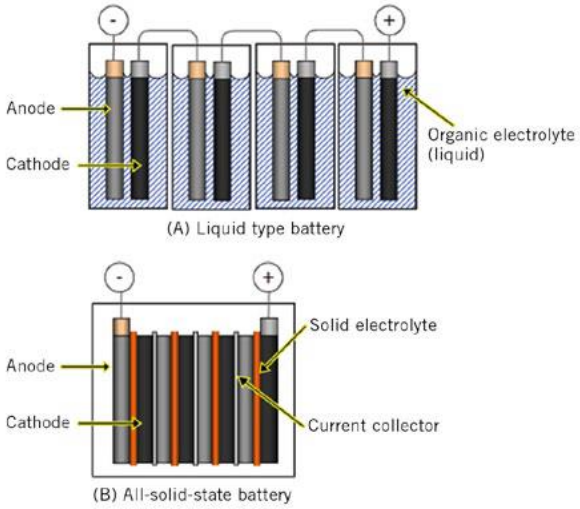

Figure 2 All-solid state battery with higher energy capacity reducing separated packaging[2]

applying complicated process which led to higher manufacturing cost and limited performances.

1.1) All-Solid State Lithium-ion Battery

All-solid state lithium-ion battery(SSE LIB) has been suggested as a solution for the safety issue of the conventional LIB. Solid-state batteries utilize solid state ion-conductive materials instead of liquid electrolyte materials. The biggest benefit from the replacement is that the solid electrolytes are safe from ignition in harsh conditions such as physical shock, contact with water, and circuit short. By resolving the safety problem, design flexibility can be increased while simplifying the manufacturing processes for the packaging. Therefore, higher energy density can

be achieved as well as reduced manufacturing cost. Thanks to this feature, solid-state lithium-ion batteries are considered as a most promising battery type for the next generation's battery system. Nowadays, a number of research groups are studying to resolve the technical challenges, yet, that exist at the SSE LIB technique.

Most of challenges for SSE LIB are arouse at electrolyte-electrode interface. As the solid electrolyte replaces liquid electrolyte, solid particles are situated between the electrodes while making a contact. As a result, the contacts between electrodes become point-contacts whereas it is surface-contacts for liquid electrolyte. Therefore, the channels where Li-ions transfer through are limited. Resultingly, large interfacial resistance is produced between electrodes and solid electrolyte, which prohibits ion-transfers and current flow[3].

1.2) Focus of Thesis

In this research, I investigated cathode and electrolyte materials to seek the optimum combinations of materials and fabrication methods, which can form a stable cell composition with reduced interfacial resistance. With each combination of cathode and electrode materials, I tested their chemical stabilities at high temperature and electrochemical properties to see their capabilities in electric cycles as battery.

For solid electrolyte, I selected $Li_{1+x}Al_xTi_{2-x}(PO_4)_3$ (LATP) based on its high ionic conductivity (10^{-3}~10^{-4} S cm^{-1} at room temperature) and good chemical stability in air and moisture. Against LATP, I tested several metal oxide cathode materials, which are lithium manganese oxide($LiMn_2O_4$), lithium iron phosphate($LiFePO_4$), lithium cobalt oxide($LiCoO_2$), lithium nickel oxide($LiNiO_4$). I chose $LiCoO_2$ (LCO) according to its conductivity after heat treatment and electrochemical property. Using LATP as electrolyte and LCO as cathode, I fabricate all-solid state device with screen printing method.

1.3) Significance of Research

Lithium-ion battery system has a great potential to be alternative powertrains for the next-generation vehicles. If developed successfully, it is expected that 7 million electric vehicles will be registered worldwide. Therefore, not only the automotive industries, but also national governments throughout the world are pursuing research on advanced energy storage system which are supposed to replace internal combustion engine vehicles. One of the main goals of projects are improving safety of battery systems while improving performance and reducing the cost per useable energy.

By utilizing solid-state electrolyte, the battery is safe from thermal runaway or ignition and no additional safety system will be required. Therefore, higher volumetric energy density can be achieved while reducing processing cost. Moreover, 3D printing manufacturing technique enables designing flexibility and is adequate for mass scale of battery production. Thus, the battery industries can extremize battery's efficiency. It is significant that studying and developing fabrication method for all solid-state lithium-ion battery with 3D printing technique will be the breakthrough for the demands that the future requires.

1.4) Overview of Thesis

This thesis includes 4 chapters. In chapter 2, experimental procedure are discussed. Recipes for each material synthesis was introduced and facilities used for material characterizations were mentioned. Procedures for stability test and cycling test were explained with governing parameters for the tests. Lastly, it covers fabrication procedures of all-solid state lithium ion cell. Chapter 3 displays data as a result of experimental methodologies from chapter 2. X-ray diffraction(XRD) patterns and scanning electron microscopy(SEM) images were provided for synthesized materials and discussed. Again, XRD patterns provided as a result of stability tests. Potential of each by-

products as component of device were discussed based on their electric conductivity referring to papers. Chapter 4 concludes and summarizes the thesis while discussing about contributions, additional applications, and future works for the research.

Chapter 2: Experimental

2.1) Materials Synthesis

Sol-gel method was used to synthesize $Li_{1.4}Al_{0.4}Ti_{1.6}(PO_4)_3$ (LATP) powders[4]. Lithium nitrate and titanium(IV) butoxide were dissolved in ethylene glycol at first. Within stirring condition, aluminum nitrate, ammonium dihydrogen phosphate, and citric acid were added to the solution. The solution was then heated at 170℃ under stirring condition at 450 rpm. Viscous gel was formed after 5 days of heating. Then, the gel was dried at 300℃, followed by sintering it at 850℃ for 5 hours to obtain the LATP powders.

Also, $LiCoO_2$ was synthesized in sol-gel method. $LiNO_3$ and Co acetate were prepared in 1.05:1 stoichiometric ratio and dissolved in water while stirring. Same molar ratio of ethylenediaminetetraacetic acid(EDTA) and citric acid was added to the solution. Heating at 220℃, the solution was stirred until the solution became gel-state. Powder was obtained after the gel was sintered at 500℃ for 12 hours[5].

$LiMn_2O_4$ precursor was synthesized in sol-gel method. First lithium chloride(LiCl) and manganese (II) chloride tetrahydrate was dissolved in 10mL water with 1.05:1 stoichiometric ratio. While stirring, citric acid and EDTA was added to the solution as chelating materials. The solution was stirred while heating at 170℃ until the solution turns to gel state. Then, the gel was dried at 450℃ for 12 hours. In this experiment, last process for the synthesis, which is heating at 850℃ was not conducted. Instead, I heated the material after when I screen printed the LMO cathode on

the LATP electrolyte pellet. In this way, I expected that I can reduce stress on the LATP pellet due to shrinkage of cathode at high temperature[4].

2.2) Material Characterization

X-ray diffraction (XRD) analysis was used to characterization for synthesized materials and materials after heat treatment. It was conducted in a θ/2θ geometry on a Rigaku's SmartLab instrument using monochromated Cu Kα radiation at 40 kV and 44 mA, receiving slit of 0.15 mm and count times of 8s/step. Data were collected in a step-scan mode in the 2θ range of 10° to 80° with intervals of 0.03°.

Also, scanning electron microscopy (SEM) was utilized for imaging synthesized material and measuring particle size. By using Hitachi S-3000 SEM at Nanotech West and Thermo Fisher's Apreo II SEM at CEMAS lab was taken for imaging the productions.

2.3) Stability Test

For all solid-state lithium-ion battery, solid electrolyte material makes contact with the solid cathode interface, which means unlike liquid electrolyte, electrolyte materials do not pervade through porous cathode material and cover cathode particles. Therefore, the particles at the interface make point contacts, where pathways for Li-ions migrations are drastically limited. It leads to a rapid decrease in ion-conductivity, which is one of the main challenge of all solid-state lithium-ion battery. One way to improve ion-conductivity is sintering the materials at high-temperature to stimulate grain growth of particles. As grain size increases, contact area between particles increases[6]. As a result, Li-ion diffusion rate increases. Moreover, thanks to the grain growth of particles at the interface, the electrode materials is able to adhere to the cathode material, which the battery cell can achieve mechanical stability. However, due to the high temperature

environment, unexpected by-product can be created because of reactions between electrode-cathode materials. These by-products can either favorably or unfavorably effect the battery cycle. Therefore, stability test is required to identify and investigate these by products and seek optimum temperatures for heat treatment.

In the experiment, electrolyte (LATP) and cathode materials were mixed in 1:1 weight ratio in powder state. The mixture was heated from 500℃ to 900℃ with 100℃ increments for 2 hours. After the heat treatment, I used X-ray diffraction(XRD) analysis for each sample to observe transition from original chemicals to another as result of reactions due to high-temperature environment. If the reaction was occurred, by-product was identified for their potential as compositions of the battery cell.

2.4) Cycling Test

Cycling tests were conducted to identify capacity and cycling ability of each combination of materials. Among the samples after the heat treatment, I focused ones who were sintered at the highest temperature but without impurities were used. It is because materials for all-solid state materials in this research are ceramics and they require high temperatures, above 700℃, to adhere each other. Therefore, I tried to find optimum temperature for electrode and cathode stick each other during the battery fabrication but without any by-products. Referred to the XRD data, I used $LiMn_2O_4$ sample heated at 700℃ and $LiCoO_2$ heated at 650℃. With the samples, I fabricated half cells using lithium hexafluorophosphate solution in ethylene carbonate and diethyl carbonate(1.0M $LiPF_6$ in EC/DEC (v:v=1:1)) as liquid electrolyte and lithium metal as anode. Liquid electrolyte was added into the cell to disregard the effect of ion conductivity of anode-electrolyte interface onto the entire cell and focus on the electrochemical properties of cathode-electrolyte active materials. The device was cycled in 0.1C rate with cut off voltage of 3.0-4.3.

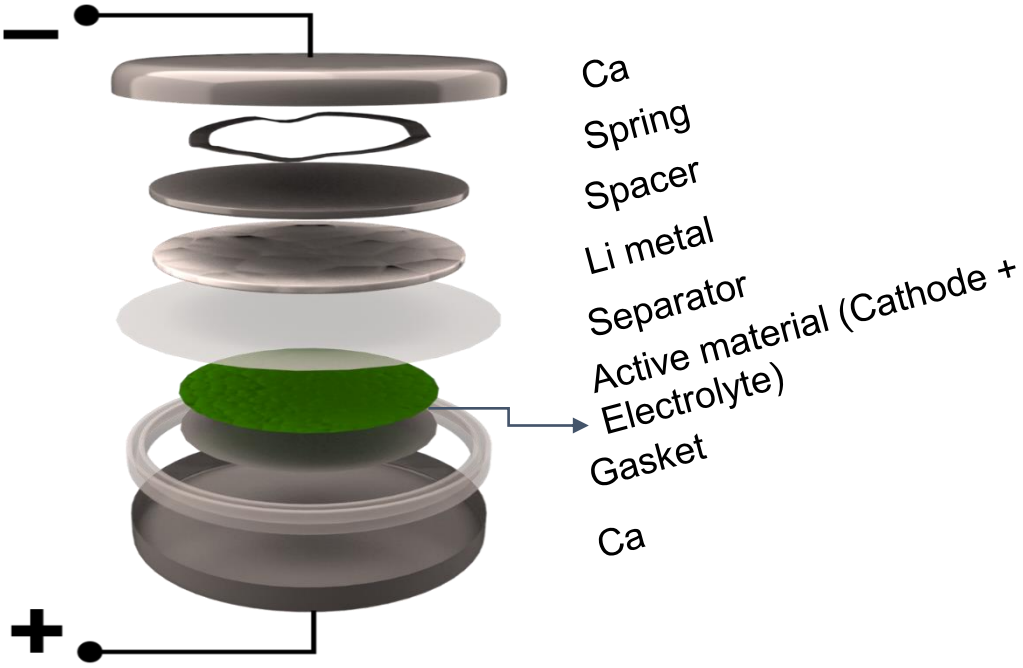

Figure 3 Explosive view of half-coin cell assembly

2.5) Fabrication of all-solid battery

Screen printing method was used to fabricate all-solid state battery. To prepare cathode in ink state, cathode materials(LMO and LCO), solid electrolyte(LATP), and binder(PVdF) was mixed in 6.7:2.7:1 weight ratio. To control the viscosity, dielectric paste was added and stirred. LATP pellet (purchased from MTI) was prepared under the mesh and the ink was screen printed on top of the LATP pellet. Then the pellet was sintered at 700°C to let the slurry adhere to the pellet. The structure, then, attached to the spacer using silver paint for convenient in assembly. The part was assembled as shown on figure 4. Likewise, liquid electrolyte was added between anode and separator to prevent conductiviy issue.

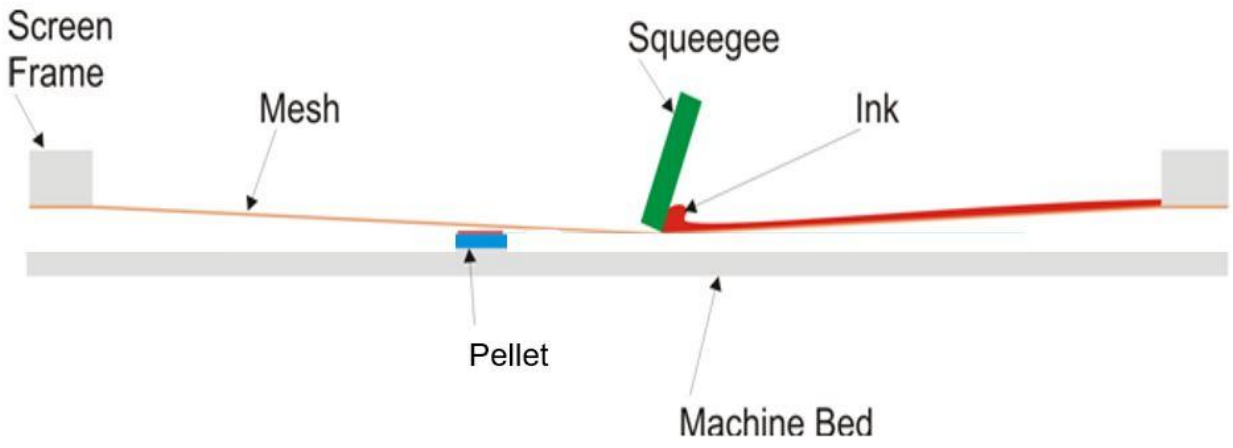

Figure 4 Schematics of screen printing cathode material ink on top of electrolyte pellet

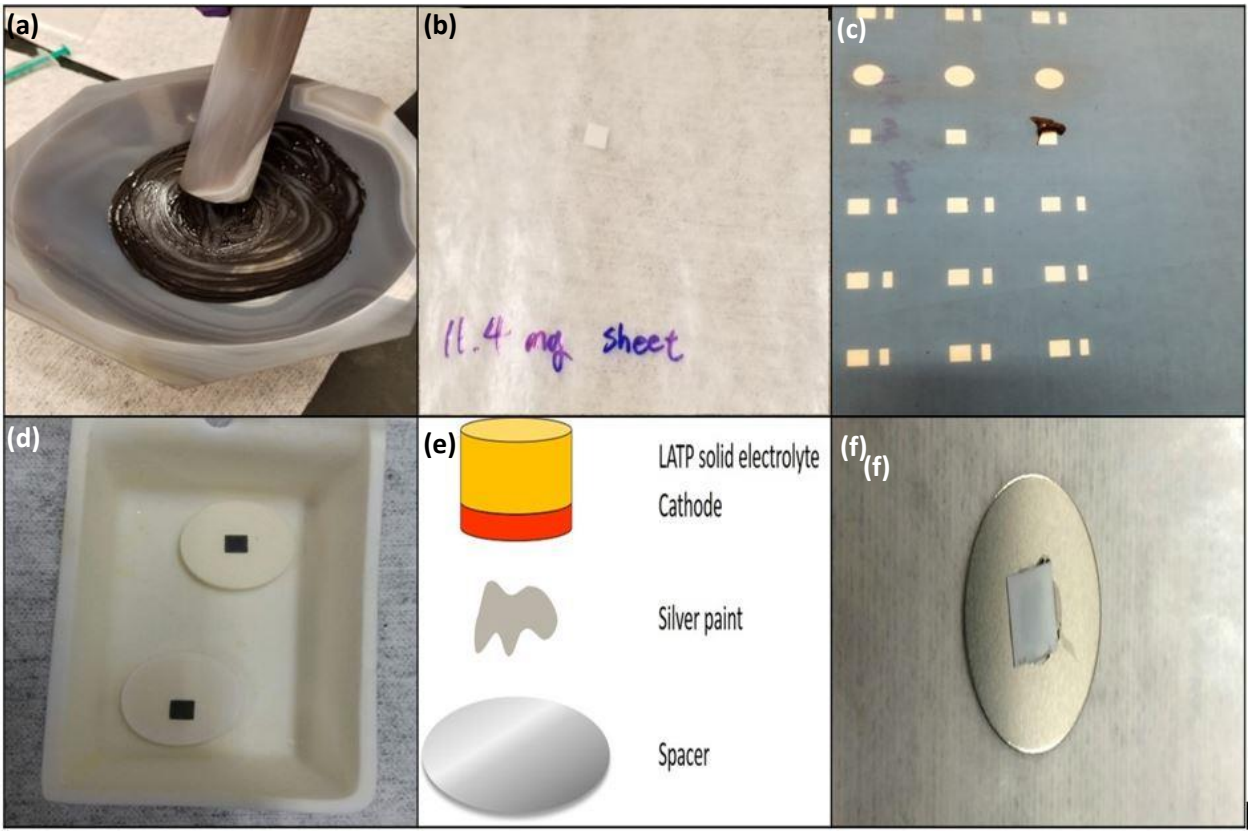

Figure 5 Procedures of fabricating All-solid state device. (a)Ink was prepared mixing cathode,electrolyte,binder and dielectric paste (b) Pellet of solid electrolyte was prepared under mesh (c) Ink was put beside mesh while pellet was placed under mesh (d) The cathode/electrolyte structure was heated at high-temperature (e)The structure was attached to the spacer using silver paint for assembly (f)Image of cathode/electrolyte/space structure before assembly

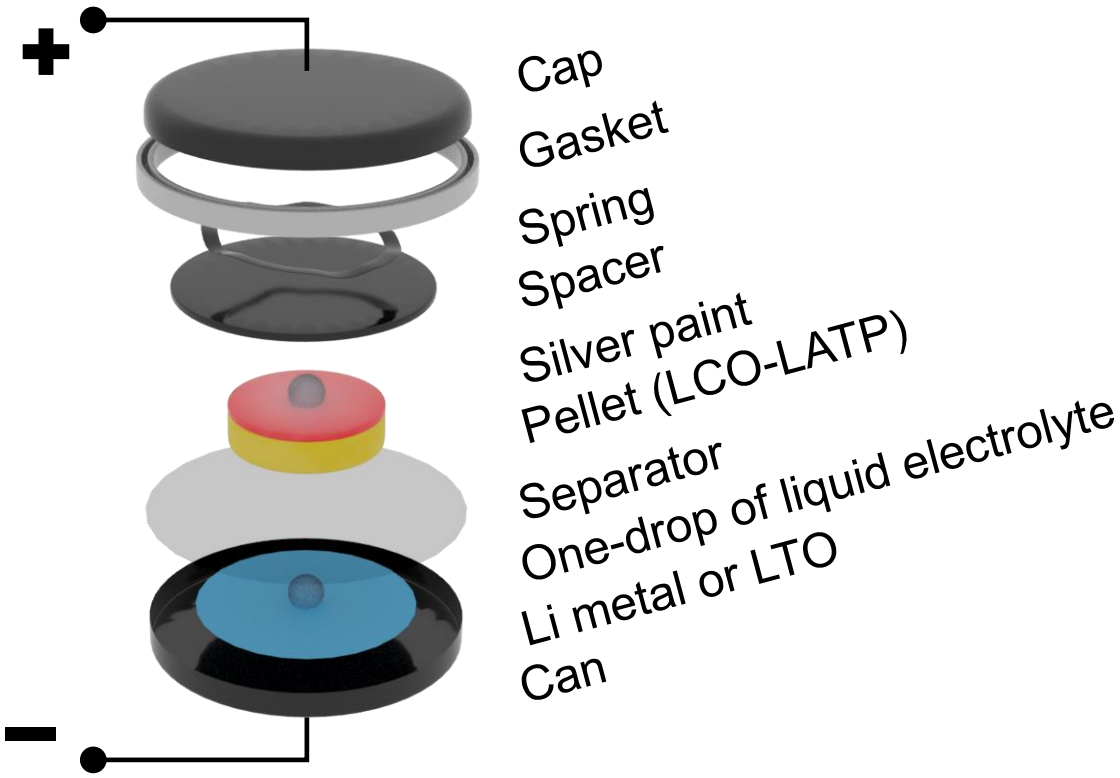

Figure 6 Explosive view for all-solid state device assembly

Chapter 3: Result and Discussion

3.1) Synthesis of Materials

$Li_{1.4}Al_{0.4}Ti_{1.6}(PO_4)_3$ (LATP) was synthesized by sol-gel method and analyzed using X-ray diffraction (XRD) (Rigaku, Smartlab at CEMAS). The XRD patterns of synthesized materials show agreement with $LiTi_2(PO_4)_3$ phase described in National Bureau of Standard (1985).[7] Also, it matches with the XRD pattern of commercialized LATP (purchased from MTI) with only minor differences. In the XRD patterns, the peaks of $AlPO_4$ phase exists around the 22^o and 35^o as an impurity phase. In the structure, it is hard to remove insulative $AlPO_4$ phase, because LATP and $AlPO_4$ composite phase is thermodynamically stable. We synthesized LATP successfully with

smaller amount of $AlPO_4$ than commercialized LATP solid electrolyte. SEM images of LATP powders were also taken with different magnifications (Figure 8). Particle sizes of LATP indicate approximately 30 μm.

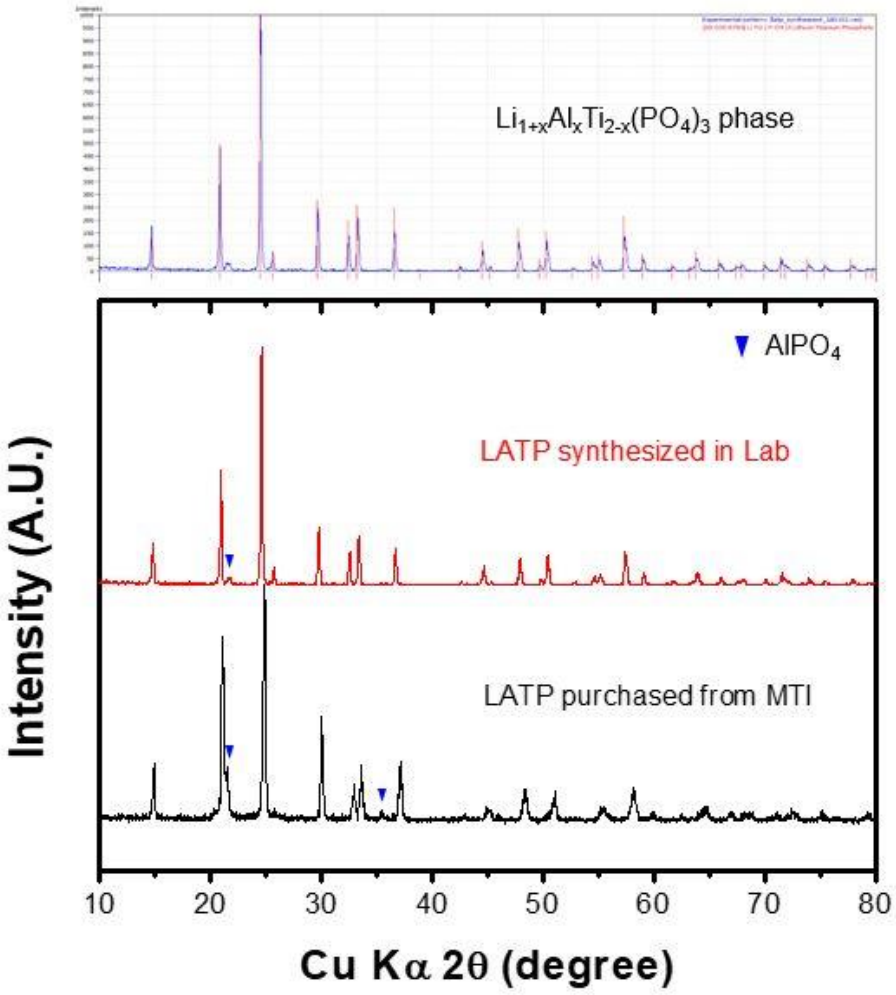

Figure 7 XRD patterns of LATP synthesized in the lab (red) and commercial LATP (black). $LiTi_2(PO_4)_3$ phase, which is a referential data, is shown on the top of this figure

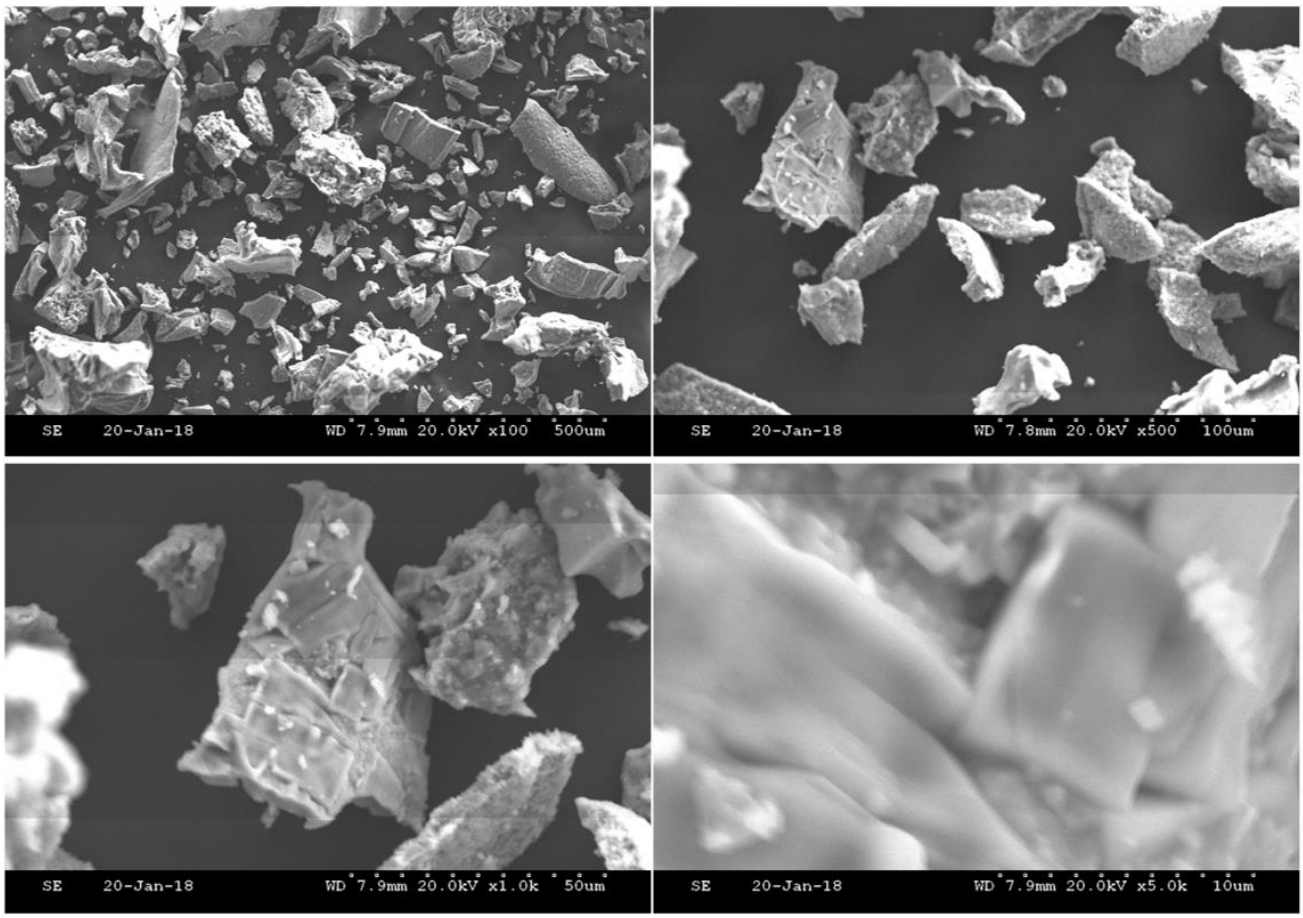

Figure 8 SEM images of $Li_{1.4}Al_{0.4}Ti_{0.6}(PO_4)_3$ synthesized by sol-gel process

$LiCoO_2$ synthesized by sol-gel method was identified by XRD. The red-peaks on the top of figure indicate reference data given from Akimoto (1998)[8], which is well-matched with XRD pattern of our sample (blue-line). The result shows we synthesized a single phase $LiCoO_2$ without any impurity phases. According to the SEM image of $LiCoO_2$ taken by Apreo II SEM, primary particle sizes are determined about to be 1 μm. Through sol-gel process, we significantly reduced particle sizes of $LiCoO_2$.

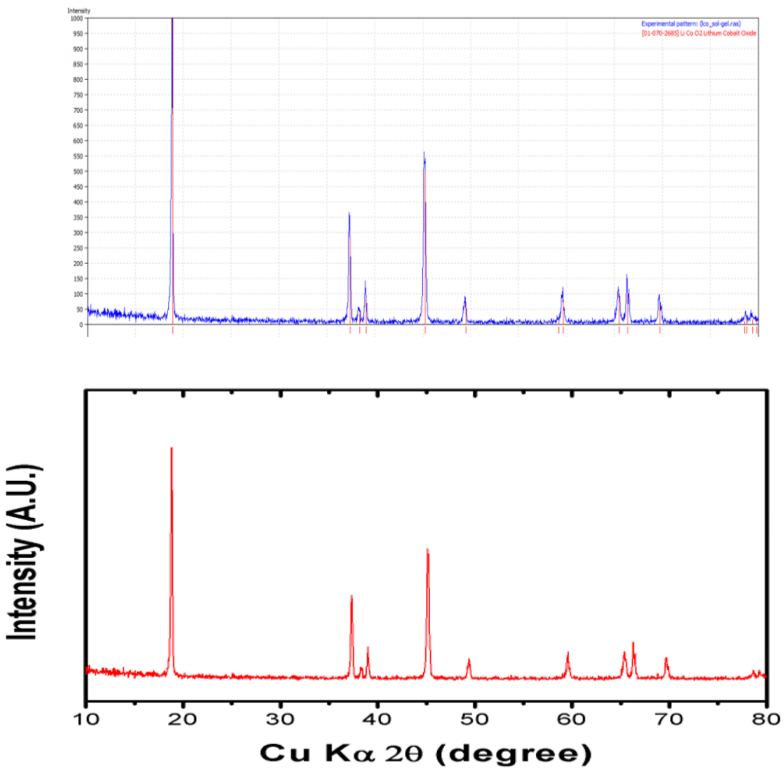

Figure 9 XRD patterns of LiCoO2 synthesized by sol-gel process. The red-peaks on the top of figure indicate the referential LiCoO2 phase

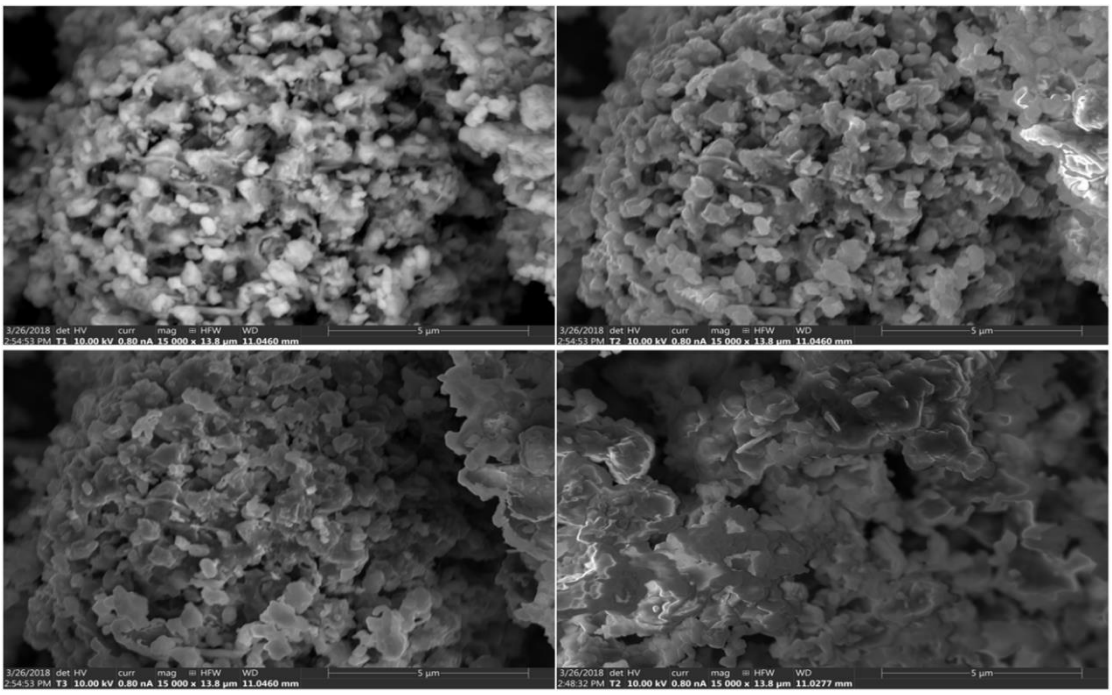

Figure 10 SEM images of $LiCoO_2$ synthesized by sol-gel process

3.2) Stability Test

In order to figure out what reaction occurs at the interface between cathode and solid electrolyte, we conducted stability test.

We started from spinel-structured $LiMn_2O_4$(LMO) cathode material for its good thermal stability. LMO powder was mixed with $Li_{1.4}Al_{0.4}Ti_{1.6}(PO_4)_3$(LATP) solid electrolyte, it then heated at different temerature. Figure 11 shows XRD patterns of mixture of LMO and LATP heated at various temperature. At the bottom of figure, XRD patterns of LMO and LATP are shown. Until 650℃, there were no change according to the heating temperature. From 700 ℃, we can observe very little amount of formation of impurity phases at around 23, 33, 38 and 56°, which was matched with Mn_2O_3 phase. In case of 800℃ samples, the peaks of Mn_2O_3 revealed more obviously, meaning the mixture was transformed to other phases with several impurities.

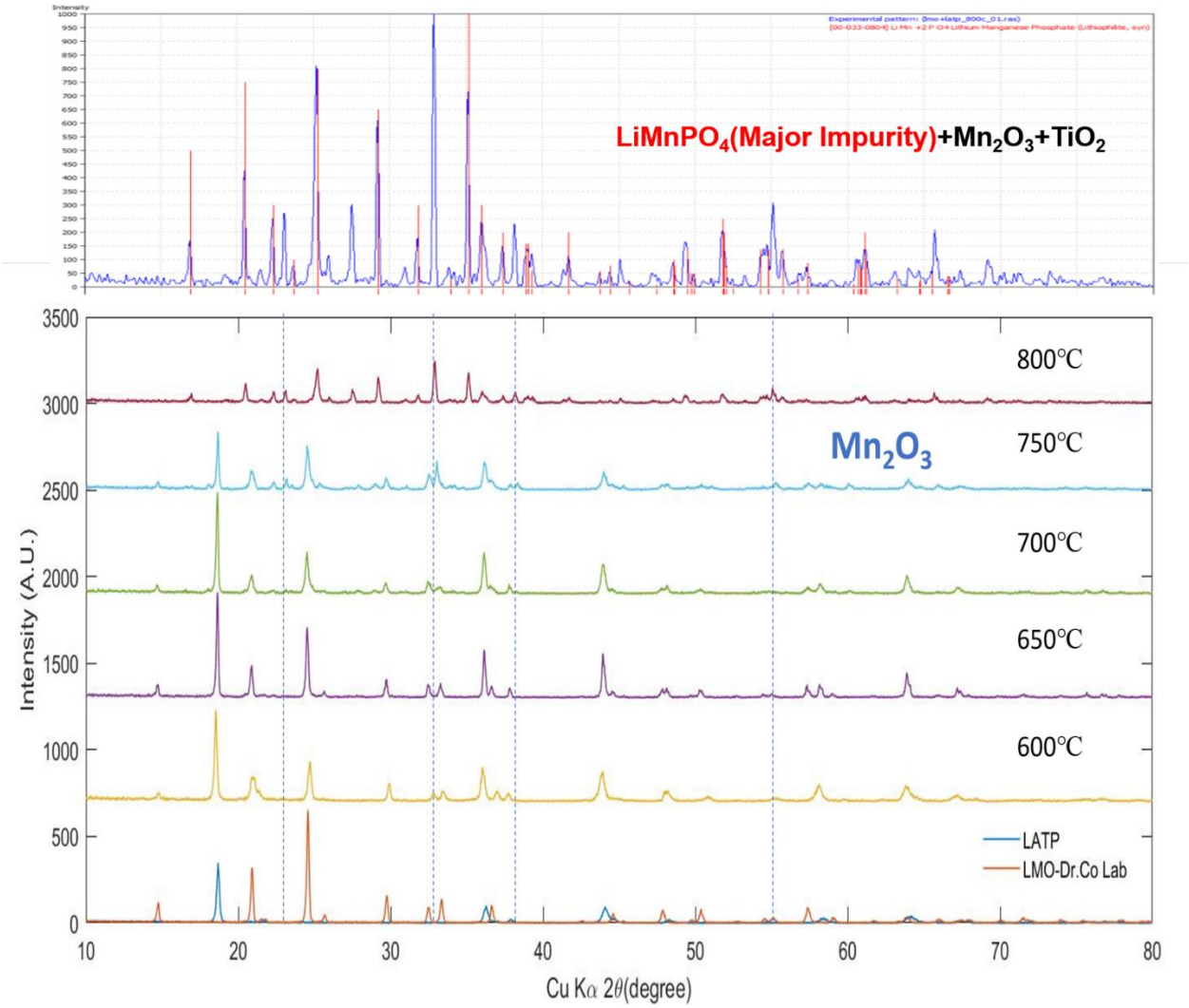

Figure 11 XRD patterns for mixture of LiMn2O4 cathode and Li1.4Al0.4Ti1.6(PO4)3 solid electrolyte at various heating temperature

At this point, we assumed that $Li_{1.4}Al_{0.4}Ti_{1.6}(PO_4)_3$ solid electrolyte generates phosphate phase when it reacts with cathode materials because of its over-amount of phosphate. So, we assumed the structure will not transform to other phase if cathode contains phosphate phase initially. We selected $LiFePO_4$ as a cathode material because it already used as a cathode material widely due to its strong stability and low-cost. In addition, both LFP and LATP are stable in Ar atmosphere at high temperature, so we expected carbon-coating, which improve electric

conductivity, is available on the cathode material. The mixture of LFP and LATP was heated from 500℃ to 900℃ with 100℃ increment. The plots show that peak changes drastically starting from 500℃. It implies that reaction occures from 500℃ and the material structure turns into a different phase. Sample for 900℃ was heated for 20 hours to make the clearer peaks. The XRD patterns for 900℃ sample matches with the patterns with $Li_3Fe_2(PO_4)_3$, according to Bykov et al.(1990)[9] After paper reviews, it is identified that ionic conductivity of $Li_3Fe_2(PO_4)_3$ is 1×10^{-8} S cm^{-1} at 300K and electric conductivity is approximately $1x10^{-6}$ S cm^{-1} at room temperature, which means the production is difficult to be utilized as a cathode material[10].

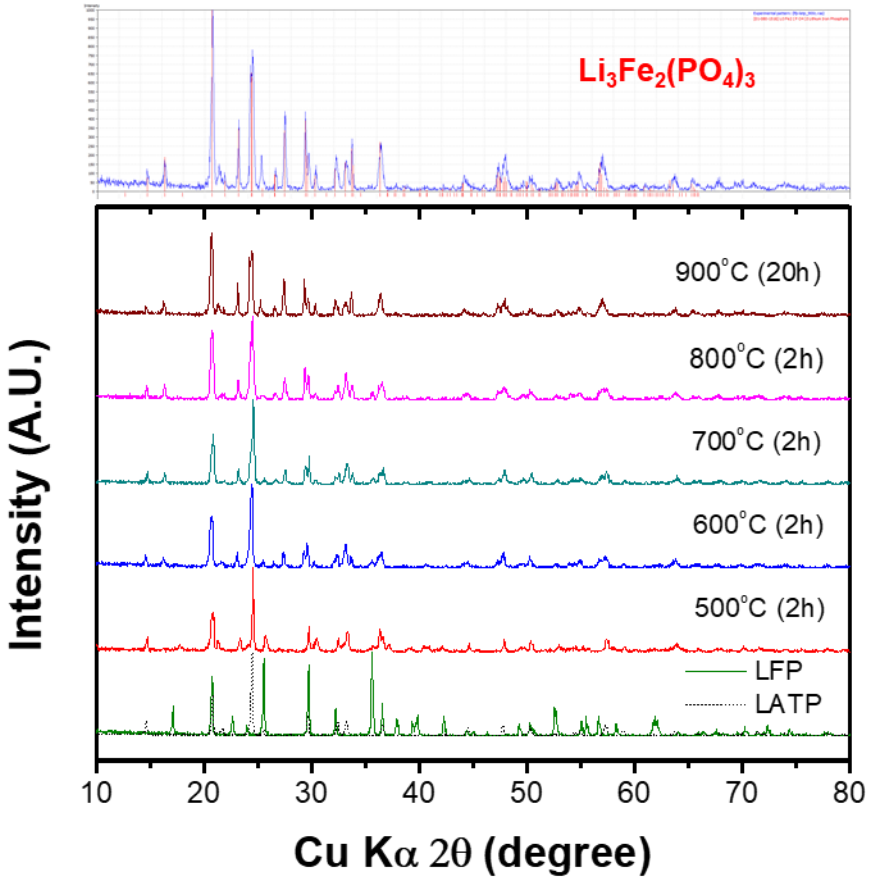

Figure 12 XRD patterns for mixture of Li3Fe2(PO4)3 cathode and Li1.4Al0.4Ti1.6(PO4)3 solid electrolyte at various heating temperature

In previous studies, we observed cathode/LATP solid electrolyte generates phosphate material at high temperature. If mixture of cathode/LATP is thermo-dynamically stable as a phosphate form at high temperature, we hypothesized $LiCoO_2$ is able to applicable to cathode material. In our assumption, $LiCoO_2$ will transform to $LiCoPO_4$ phase when it reacts LATP solid electrolyte. $LiCoPO_4$ is one of promising material for cathode since it reacts around 4.8 V and the discharge capacity of $LiCoPO_4$ cathode indicates around 130 mAh g-1 at 0.1 C-rate current[11].

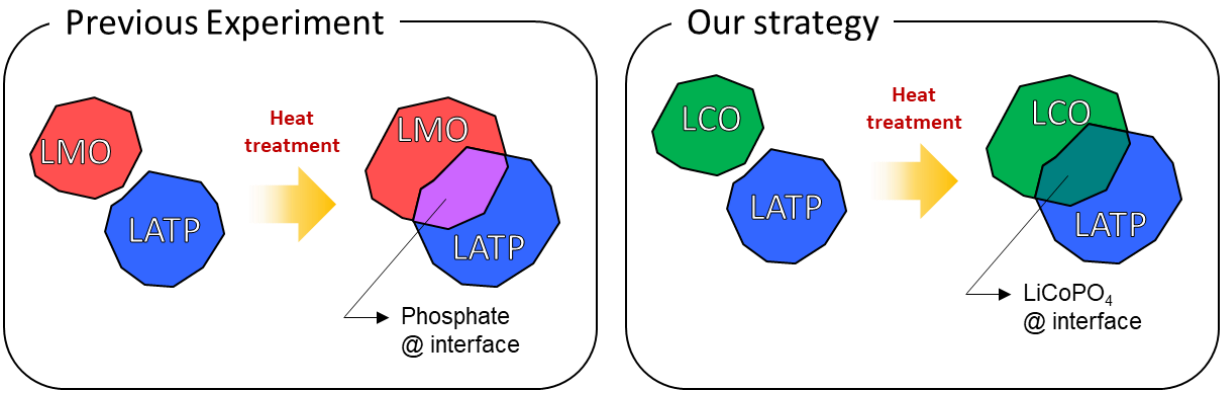

Figure 13 Schematic images of concept for our approach using $LiCoO_2$ cathode to make high-voltage $LiCoPO_4$ cathode material

So, we approached to heat mixture of $LiCoO_2$ and $Li_{1.4}Al_{0.4}Ti_{1.6}(PO_4)_3$ at different temperature (see Figure 14). Until 600 ^oC, the structural changes were not observed by XRD. However, from 650 ^oC, very small amount of Co_3O_4 was revealed and it grew according to increase of heating temperature. At high temperature, mixture of LCO and LATP was transformed to the $LiCoPO_4$, Co_3O_4 and TiO_2 phases, which is exactly same with our assumption.

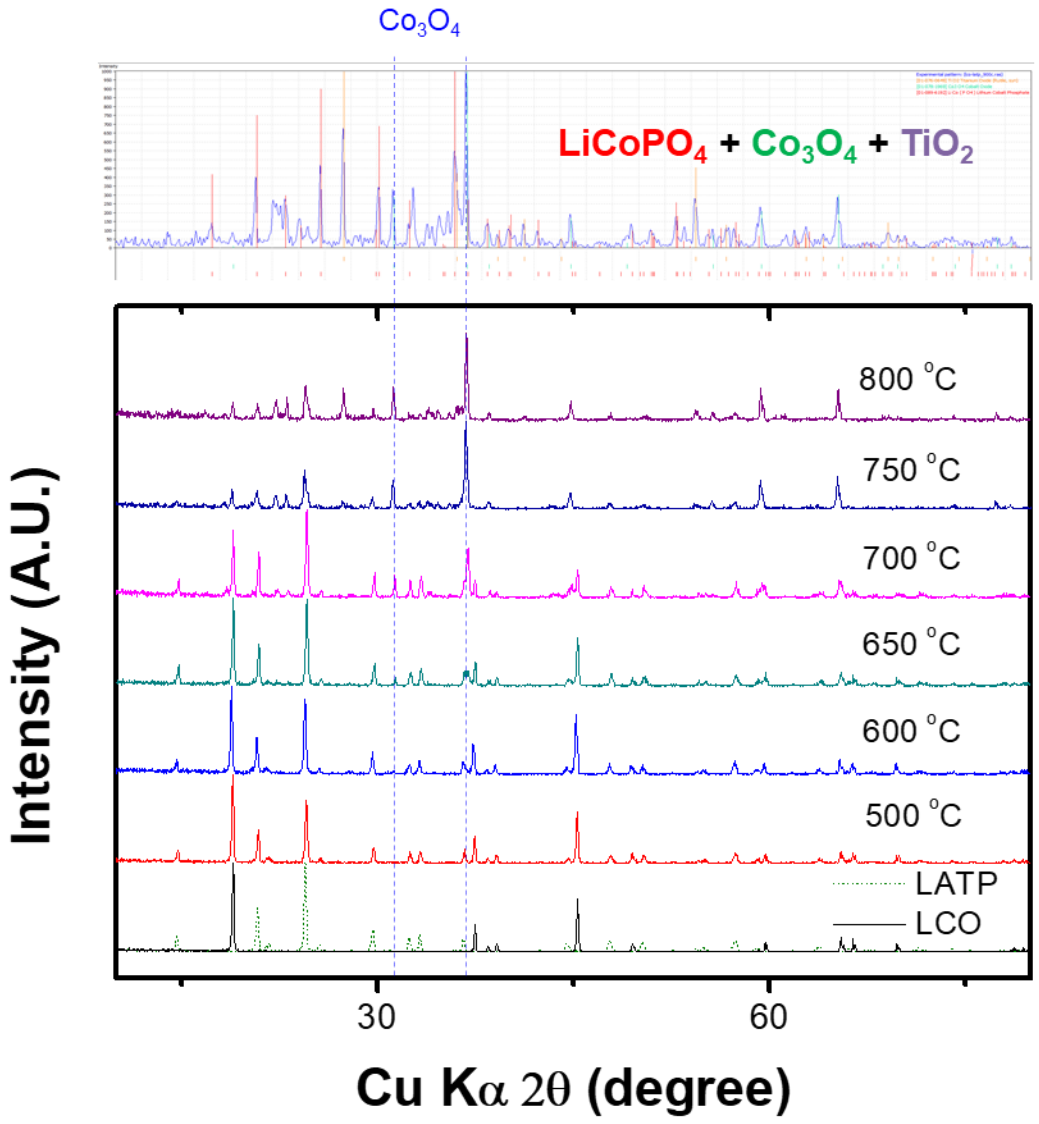

Figure 14 XRD patterns for mixture of LiCoO2 cathode and Li1.4Al0.4Ti1.6(PO4)3 solid electrolyte at various heating temperature

On the table 1, electric conductivities of various by-products are presented. Since mixture of LMO/LATP creates insulative Mn_2O_3 from 700 °C and $LiMnPO_4$ from 800 °C, it is hard to apply to a cathode material for solid-state battery. The by-product, $Li_3Fe_2(PO_4)_3$, shows poor electric conductivity of $1x10^{-6}$ S cm^{-1}, meaning it is not applicable to battery devices[11]. A good

sign is that electric conductivity of Co_3O_4 indicates semi-conductive property, which means it is applicable to solid-state battery device[12].

Table 1 Electric conductivities of by-products at room temperature

By-product	Electric Conductivity (S cm^{-1})	Reference
$LiMnPO_4$	1×10^{-10}	[13]
Mn_2O_3	5×10^{-5}	[14]
$Li_3Fe_2(PO_4)_3$	1×10^{-6}	[11]
$LiCoPO_4$	1×10^{-9}	[15]
Co_3O_4	1×10^{-3}	[12]

3.3) Cycling Test

Figure 16 shows charge and discharge curves of coin-type cell that used mixture of LMO-LATP heated at 700℃ as a cathode. Liquid electrolyte and lithium metal anode to simply check feasibility as an electrochemical cell. The initial charge capacity of it indicates 43 mAh g^{-1}, but it soon decreased around 2 mAh g^{-1} from second cycle. It is hard to determine the exact reason why the capacity fading occurs at the initial charge, but we can conclude that it is not utilizable to cathode material because of its low capacity. And we can assume that the low capacity comes from the low electric conductivity of Mn_2O_3 impurity.

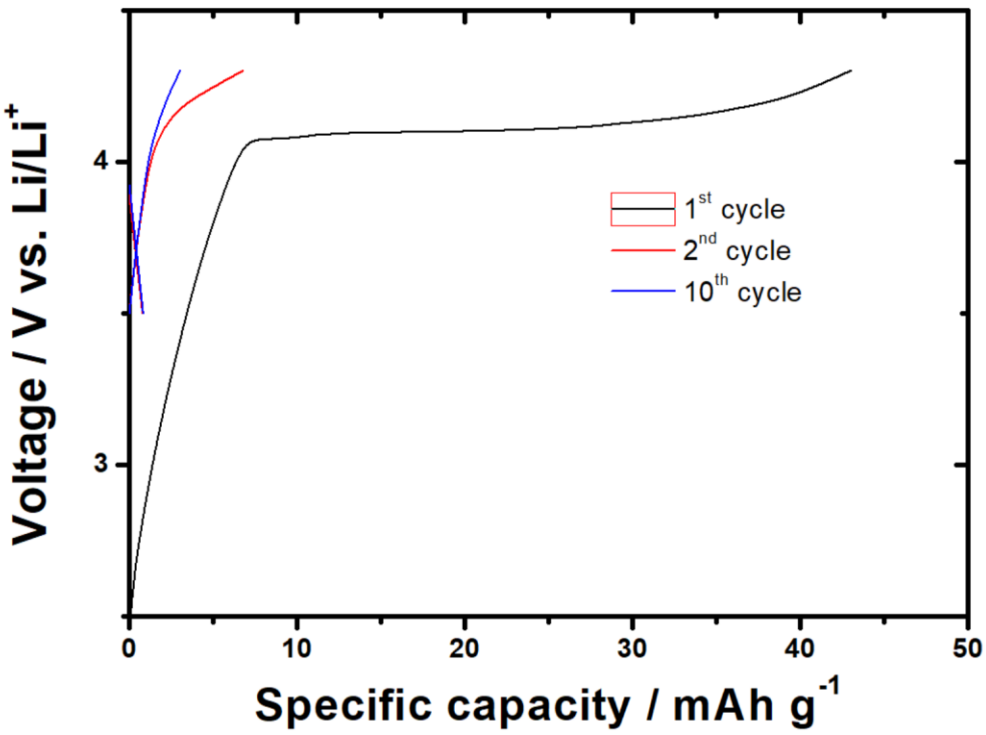

Figure 15 Charge-discharge curves of LMO-LATP composite cathode battery that uses 1M LiPF6 EC:DEC solvent as an electrolyte and Li metal as an anode

LFP-LATP composite was also tested as electrochemical cell. In previous studies, LFP-LATP composite transformed to $Li_3Fe_2(PO_4)_3$ at high temperature and from table 1, we could know it is one of insulator. Figure 16 shows charge and discharge capacity of $Li_3Fe_2(PO_4)_3$ cathode cell operated in liquid electrolyte system. Discharge capacities of it were recorded below 1 mAh g^{-1}, which means it is not applicable. We hypothesize the poor capacity is attributed from the poor electric conductivity of $Li_3Fe_2(PO_4)_3$. In our hypothesis, since the electrode cannot deliver electrons to Al current collector, it did not work well.

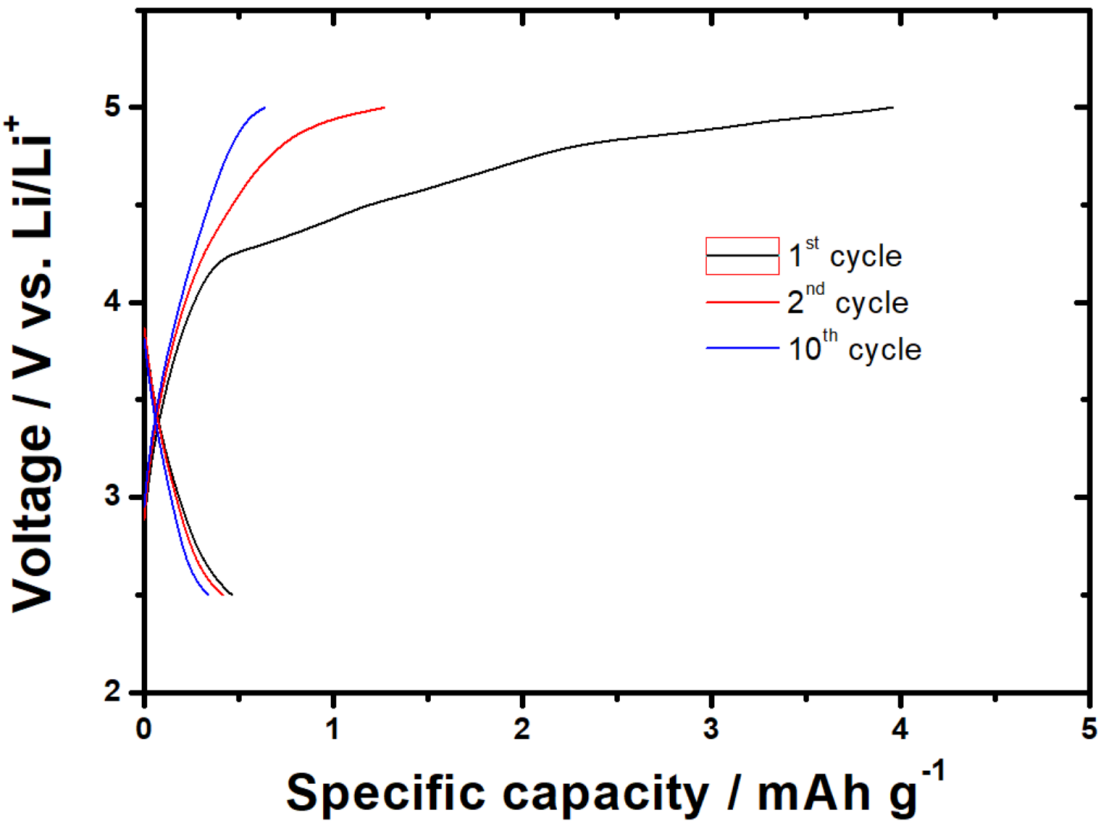

Figure 16 Charge-discharge curves of LFP-LATP composite cathode battery that uses 1M LiPF6 EC:DEC solvent as an electrolyte and Li metal as an anode

In the XRD patterns of mixture of LCO-LATP, Co_3O_4 phase was formed at 650℃, 700℃, and 750℃ as an impurity phases. Co_3O_4 is known as semi-conductor that can help behavior of electrons move smoothly[12]. So, the LCO-LATP composite was electrochemically evaluated in the liquid electrolyte system to briefly check the electrochemistry. LCO-LATP composite heated at 750℃ indicated very poor electrochemical performance which is shown in Figure 18(a). The discharge capacities of the sample heated at 750℃ shows below 2 mAh g^{-1}. In terms of 700℃ sample, it also shows poor capacity of around 40 mAh g^{-1}. For the 650℃ sample, it shows significant improvement, capacity around 125 mAh g^{-1}, which means it can be utilizable to solid-state battery.

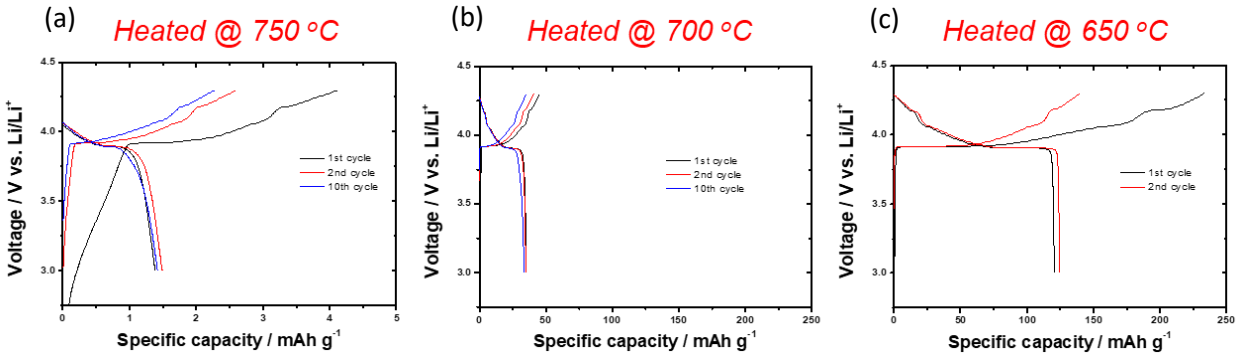

Figure 17 Charge-discharge curves of LCO-LATP composite cathode cell according to different heating temperature of 650-750℃

3.4) Fabrication of All-Solid State Device

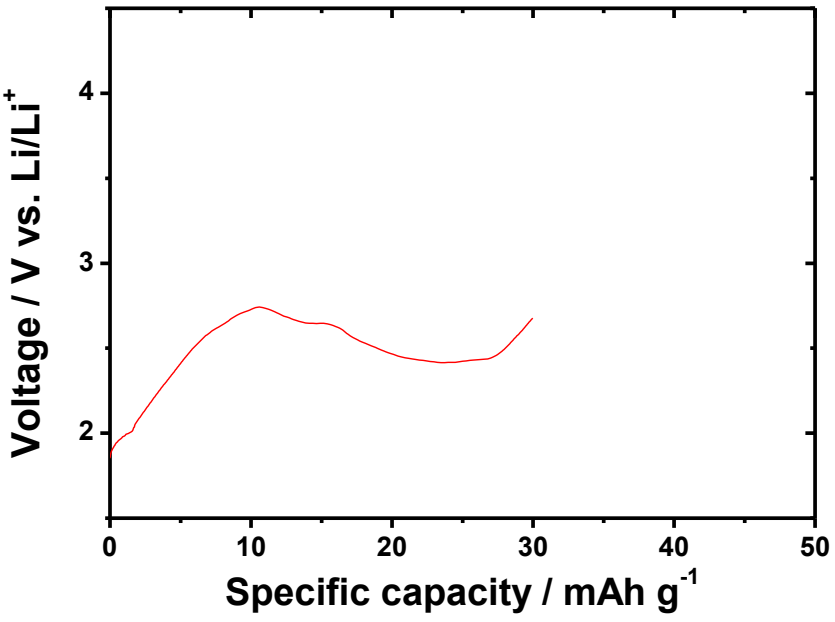

Figure 18 Cycle result of LCO-LATP all-solid state device heated at 650 ℃

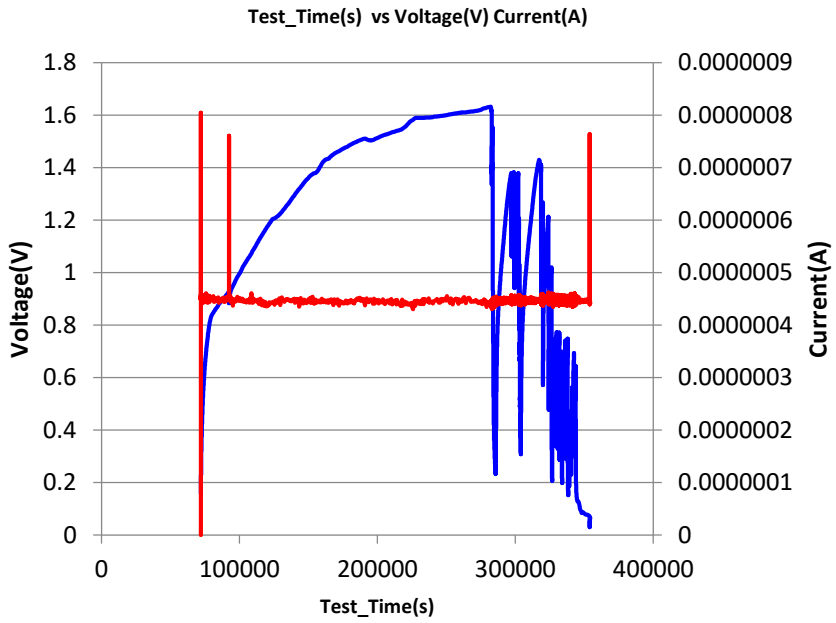

Figure 19 Charge-discharge curves of LCO-LATP all-solid state device heated at 650 ℃

All-solid state lithium-ion battery fabricated by $LiCoO_2$ as cathode and $Li_{1.4}Al_{0.4}Ti_{1.6}(PO_4)_3$ with the heat treatment temperature of 650℃. Resulting voltage and current plot showed poor performance with energy capacity about 30 mAh/g and voltage and current cycling plots look collapsing overtime(Figure 19).

We suggested a few possible causes for poor cycling ability. First probable reasoning is decomposition of organic binder in the silver paste at high-voltage environment. According to the charge-discharge plot from the cycling of ASS LIB(Figure 18), the plot does not form a plateau like charge-discharge curves from the cycles of half-cell heated at 650℃ (Figure 17(c)). Therefore, we can consider that certain chemical is decomposed during the cycles. Silver paste is the most likely to have decomposition because it includes binder materials. Organic binder might have led to low electric conductivity between the cathode and spacer as it decomposes. For the further experiments, nickel mesh or traditional binder such as polyvinylidene fluoride(PVDF) can be utilized since their properties are already known to be conductive and stable at high-voltage.

Another factor caused poor performance is low sintering temperature for cathode-electrolyte component. The heating temperature might not have provided sufficient contact between cathode and electrolyte and therefore, resulted in low ionic and electric conductivity between cathode and electrolyte. After finishing the cycle, the coin cell was disassembled and adherence of cathode was tested using tape. By checking that the cathode was easily fell off from the electrolyte, we could identify that the contact between cathode-electrolyte interface is not enough. Even though we have considered a few factors of failure, we need data generalization and optimization to clearly verify the dominant factor.

Chapter 4: Conclusions

The purpose of this project was to explore material combinations of cathode and electrolyte materials to seek optimum chemicals and methods for the fabrications of all-solid state lithium-ion battery with proper electrochemical property.

4.1) Summary

Selecting $Li_{1.4}Al_{0.4}Ti_{1.6}(PO_4)_3$ as solid electrolyte material, $LiMn_2PO_4$ (LMO) was tested as cathode material, firstly. As a result of heat treatment, it is identified materials turns to phosphate structure due to thermos-stabilities of phosphate phases. Therefore, we tried $LiFePO_4$ for cathode because of its phosphate abundance. However, $Li_3Fe_2(PO_4)_3$ was formed after heat treatment and the conductivity of material was too low for the battery performance. Hypothesizing phosphate phase will be produced after heat treatment, we tested $LiCoO_2$ for cathode material, expecting $LiCoPO_4$ will be produced since $LiCoPO_4$ is known as high voltage cathode material. After cycling of each material combination, $LiCoO_2$-LATP heated at 650℃ showed the best result with energy capacity of 125 mAh g^{-1}. Accordingly, all-solid state lithium-ion battery was fabricated using

$LiCoO_2$ as cathode material with heat temperature at 650℃. The cycling resulted in poor battery performance with capacity of 0.01 mAh g^{-1}.

4.2) Contribution

Battery technology involves various fields such as chemistry, material science and engineering, and electrical engineering. Especially, characteristics of material science is profound for this experiment. That is, chemical phenomenon is difficult to simulate because it is almost impossible to quantify chemical characteristics of each material. Therefore, experiment procedures are somewhat iterative and repetitive. I believe information from thesis can contribute as data for future researches.

4.3) Additional Application and Future Work

For the optimization, same materials and parameters will be used to fabricate additional devices. To improve conductivity, graphite power will be added to the cathode ink as conductive agent. Also, precision during the fabrication of device needs to be improved for the optimization. One way is using viscometer to retain the uniform viscosity and thickness of ink on the substrate.

Furthermore, I can test other cathode and electrolyte materials using the skills and knowledge I obtained throughout this research. I can conduct tests in similar way that I did for the materials in this project and I will be available to process new data in the other applications.

Appendix

1) XRD Analysis

X-ray diffraction methods are analyzing technology for determining the crystal structure of materials. This characterization technique utilizes high-energy electron beam to excite electrons in the inner shell of target atom (Cu in this experiment). Then, transitions of outer-shell electrons to the inner-shell vacancies generate X-ray beam where it is radiated to the sample. The incident X-ray beams are diffracted on a crystalline solid sample and the phase difference of electromagnetic waves after the diffraction can be result in either constructive or destructive interference. The diffracted waves are read by detector and the patterns calculated based on Bragg's Law

$$n\lambda = 2dsin\theta$$

$\lambda =$ wavelength of incident beam

$\mathrm{d} =$ plance spacing

$\theta =$ angle of incident beam

$$d_{hkl} = \frac{a}{\sqrt{h^2 + k^2 + l^2}}$$

Since the lattice parameter(a) and Miller indices (hkl) are differently calculated by each characteristic crystal structure of materials, the diffraction patterns of crystallographic planes can be represented for each incident angles[16] .

In this projected, $K_{\alpha 1}$ beam from copper was used to analyze sintered cathode-electrolyte mixtures.

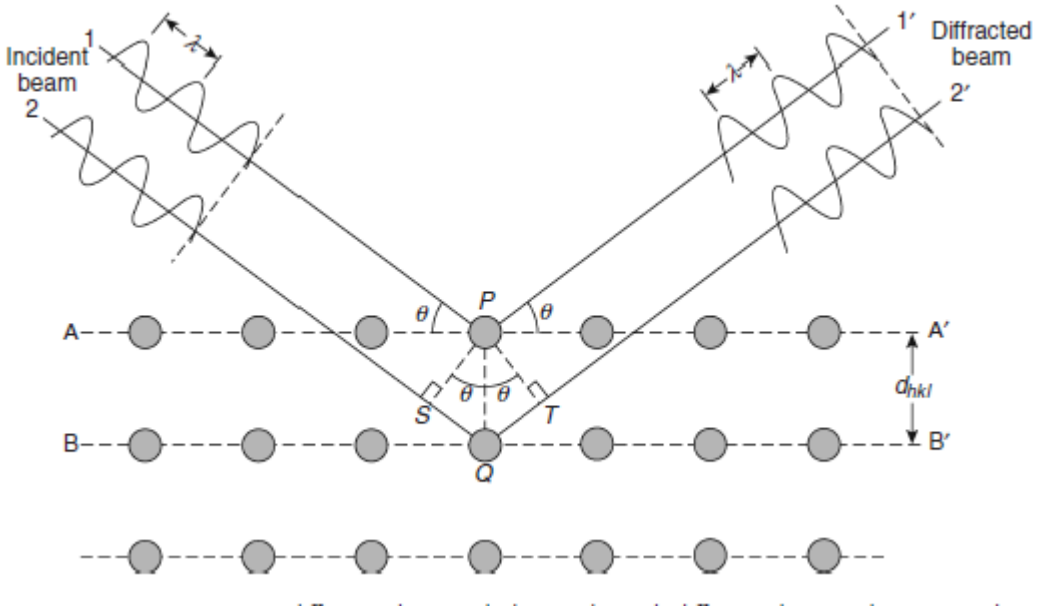

Figure 20 Schematics of X-ray beams diffract off of the crystal structure

Reference

[1] J. G. Kim et al., “A review of lithium and non-lithium based solid state batteries,” Journal of Power Sources, vol. 282, pp. 299–322, May 2015.

[2] C. Yada and C. Brasse, “Better batteries with Solid-state instead of liquid-based electrolytes,” ATZelektronik worldwide, vol. 9, no. 3, pp. 10–15, 2014.

[3] M. Gellert et al., “Charge Transfer across the Interface between LiNi0.5Mn1.5O4 High-Voltage Cathode Films and Solid Electrolyte Films,” J. Electrochem. Soc., vol. 162, no. 4, pp. A754–A759, Jan. 2015.

[4] S.-D. Lee et al., “Composite Electrolyte for All-Solid-State Lithium Batteries: Low-Temperature Fabrication and Conductivity Enhancement,” ChemSusChem, vol. 10, no. 10, pp. 2175–2181, May 2017.

[5] A. Feldhoff, M. Arnold, J. Martynczuk, T. M. Gesing, and H. Wang, “The sol–gel synthesis of perovskites by an EDTA/citrate complexing method involves nanoscale solid state reactions,” Solid State Sciences, vol. 10, no. 6, pp. 689–701, Jun. 2008.

[6] M. Faryna, P. Bobrowski, Z. Pędzich, and M. Bućko, “Correlation between microstructure and ionic conductivity in cubic zirconia polycrystals,” Materials Letters, vol. 161, pp. 352–354, Dec. 2015.

[7] Natl. Bur. Stand. (U.S.) Monogr. 25 21, 79 (1985)

[8] J. Akimoto, Y. Gotoh, and Y. Oosawa, “Synthesis and Structure Refinement of LiCoO2Single Crystals,” Journal of Solid State Chemistry, vol. 141, no. 1, pp. 298–302, Nov. 1998.

[9] A. B. Bykov et al., “Superionic conductors Li3M2(PO4)3 (M□Fe, Sc, Cr): Synthesis, structure and electrophysical properties,” Solid State Ionics, vol. 38, no. 1, pp. 31–52, Apr. 1990.

[10] K. Nagamine, K. Hirose, T. Honma, and T. Komatsu, “Lithium ion conductive glass–ceramics with Li3Fe2(PO4)3 and YAG laser-induced local crystallization in lithium iron phosphate glasses,” Solid State Ionics, vol. 179, no. 13, pp. 508–515, Jun. 2008.

[11] D. Choi et al., “LiCoPO4 cathode from a CoHPO4·xH2O nanoplate precursor for high voltage Li-ion batteries,” Heliyon, vol. 2, no. 2, p. e00081, Jan. 2016.

[12] C. A. Antonyraj, D. N. Srivastava, G. P. Mane, S. Sankaranarayanan, A. Vinu, and K. Srinivasan, “Co3O4 microcubes with exceptionally high conductivity using a CoAl layered double hydroxide precursor via soft chemically synthesized cobalt carbonate,” J. Mater. Chem. A, vol. 2, no. 18, pp. 6301–6304, Apr. 2014.

[13] Y. Dong, Y. Zhao, H. Duan, and Z. Liang, “Enhanced electrochemical performance of LiMnPO4 by Li+-conductive Li3VO4 surface coatings,” Electrochimica Acta, vol. 132, pp. 244–250, Jun. 2014.

[14] F. Hong, B. Yue, N. Hirao, Z. Liu, and B. Chen, “Significant improvement in Mn2O3 transition metal oxide electrical conductivity via high pressure,” Scientific Reports, vol. 7, p. 44078, Mar. 2017

[15] J. Wolfenstine, “Electrical conductivity of doped LiCoPO4,” Journal of Power Sources, vol. 158, no. 2, pp. 1431–1435, Aug. 2006.

[16] Cullity, B.D. and Stock, S.R. (2001) Elements of X-Ray Diffraction, 3rd edn, Prentice Hall, Upper Saddle River, NJ.